

SupplementalMaterial

Appendix S1.

Mud (mode 52-60 μm ; Appendix II) was collected from a modern lake (Oklahoma) and frozen at -15°C overnight. After preliminary tests of the impact of sediment depth (1-10 mm in 90 mm and 48 mm-diameter petri dishes), and sediment homogeneity (sieved vs. un-sieved), all experiments used sieved sediment (mode 52-60 μm), \sim 1-10 mm deep. Sediment depths did not impact morphology. Experimental variables in this study included (1) solution chemistry: distilled water + NaCl (0%, 0.1%, 0.5%, 1%), and (2) sediment saturation: saturated vs. supersaturated. Saturation was achieved by addition of solution to sediment until pore spaces were full; supersaturation indicates that ≤ 1.5 mm films of solution existing atop the sediment surface. Models with dilute NaCl solutions were performed to test the effect of the presence of salts on morphology. We did not simulate growth of evaporitic minerals (e.g. calcium sulfates like gypsum) in sediment due to their moderate-to-low solubility, the time required to grow well-formed crystals (up to a year), uncertainty around paleoclimate-specific variables (e.g. availability of organics, sediment composition), and because such experiments are already well-documented in the literature (e.g. Cody and Cody, 1988; Magee, 1991). Grain size, temperature, and time were held constant in all experiments.

Appendix S2.

Grain size distribution of mud used for laboratory simulation of ice crystal growth after being sieved (mode 52-60 μm ; *blue*) and grain size distribution of disaggregated Usclas Formation mudstone (mode 20-45 μm ; *black*).

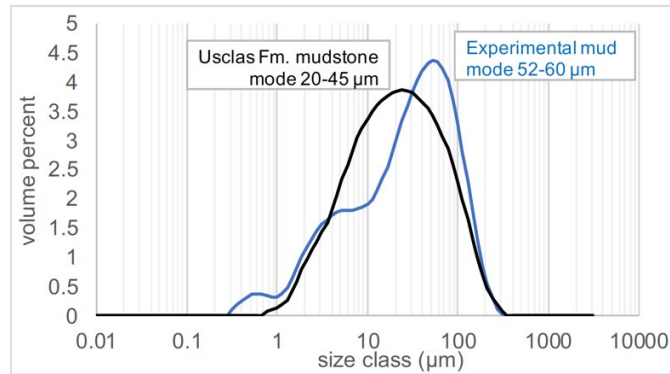


Figure S1

Appendix S3.

Select photos from the literature of markings interpreted as ice crystals in strata from various geologic intervals (**Figure S2**; following page). *See also*: Table 1 from main text. References cited for these photos and for Table I (main text) are listed below. Photo descriptions in order as follows: (A) Modern, casts of ice crystals in loess, IL, U.S. (Udden, 1918), (B) Modern, in mud, Capitol Reef National Park, UT, U.S. (Photo by K. Benison, 2010), (C) Modern, in playa lake, western Argentina (Photo by G.S. Soreghan), (D-E) Late Pleistocene, in fine sands, UT, U.S. (from Mark, 1932), (F) Pleistocene, reticulate-chaotic cryostructures in ice-rich, lake-bottom muds (from French and Shur, 2010), (G) Middle-Permian, in Carlsbad limestone, Guadalupe Mts., U.S. (from Lang, 1937), (H-I) Upper Cretaceous, in Eagleford limestone – clays, TX, U.S. (from Udden, 1918), (J) Upper Ordovician, in sand-mud, Morocco (from Nutz et al., 2013), (K) Upper Ordovician, in mud, Libya (from Girard et al., 2015), (L) Lower Carboniferous, in mud-silt, De L'aïr, Niger (from Lang et al., 1991).

- Allan, J.A., 1926, Ice Crystal Markings: *The American Journal of Science*, s. 5, v. 11, p. 494-500.
- Clarke, J.M., 1918, Strand and Undertow Markings of Upper Devonian Time as Indications of the Prevailing climate, *New York State Museum Bulletin*, p. 199–210.
- Dionne, J.C., 1985, Formes, figures et facies sédimentaires glaciels des estrans vaseux des régions froids, *Palaeogeography, Palaeoclimatology, Palaeoecology*, v. 51, p. 415–451.
- French, H., and Shur, Y., 2010, The principles of cryostratigraphy. *Earth-Science Reviews*, v. 101, n. 3–4, p. 190–206. <https://doi.org/10.1016/j.earscirev.2010.04.002>

- Girard, F., Ghienne, J., Du-bernard, X., and Rubino, J., 2015, Sedimentary imprints of former ice-sheet margins : Insights from an end-Ordovician archive (SW Libya), *Earth Science Reviews*, v. 148, p. 259–289. <https://doi.org/10.1016/j.earscirev.2015.06.006>
- Hänzschel, W., 1935, Recent ice crystals in marine sediments and fossil traces of ice crystals, *Senckenbergiana*, v. 17, p. 151-177.
- Lang, P.J., Dijon, M., Yahaya, M., El Hamet, M.O., and Besombes, J.C.M., 1991, Depots glaciaires du Carbonifere inferieur a l'Ouest de l'Air (Niger). *Geologische Rundschau*, v. 80, n. 3, p. 611–622.
- Lang, W.B., 1937, The Permian Formations of the Pecos Valley of New Mexico and Texas, *Bulletin of the American Association of Petroleum Geologists*, v. 21, n. 7, p. 833–898.
- Mark, W.D., 1932, Fossil Impressions of Ice Crystals in Lake Bonneville Beds, *The Journal of Geology*, v. 40, n. 2, p. 171–176.
- Nutz, A., Ghienne, J., and Storch, P., 2013, Circular, cryogenic structures from the hirnantian deglaciation sequence (Anti-Atlas, Morocco), *Journal of Sedimentary Research*, v. 83, p. 115–131. <https://doi.org/10.2110/JSR.2013.11>
- Reineck, H.E., 1955, Marken, Spuren und Fährten in den Waderner Schichten (ro) bei Martinstein/Nahe, *Neues Jb. Geol. Palaont. Abh.*, v. 101, p. 75-90.
- Reineck, H.E., and Singh, I.B., 1980, *Depositional sedimentary environments*. Springer-Verlag, Berlin, p. 551.
- Shaler, N.S., Woodworth, J.B., and Marbut, C.F., 1806, The glacial brick of Rhode Island and Sotheastern Massachusetts, 17th annual report, director US Geological Survey, p. 951.
- Udden, J.A., 1918, Fossil Ice Crystals, *University of Texas Bulletin*, n. 1821, p. 3–39.

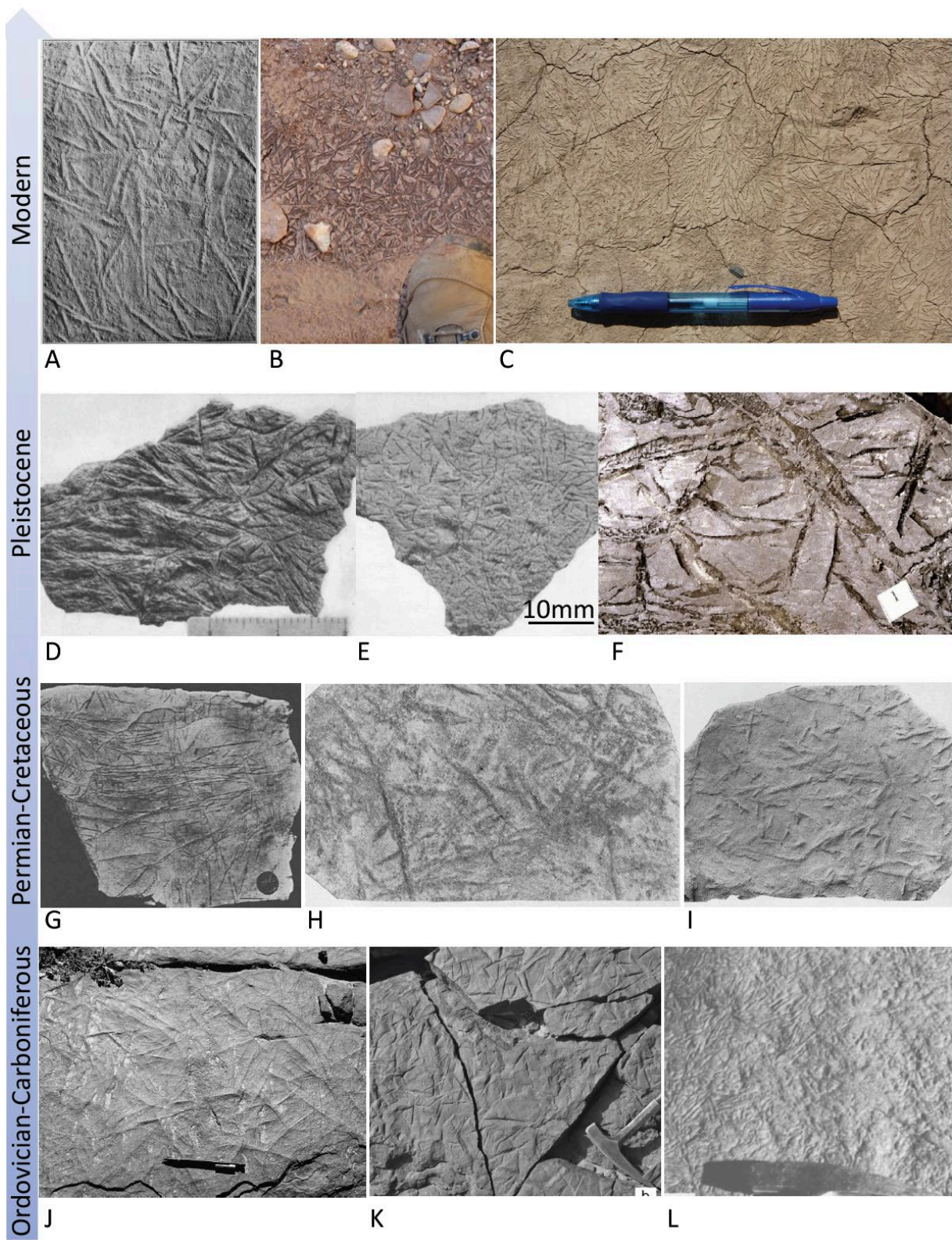


Figure S2

Appendix S4.

Select photos from the literature of rare forms of several minerals or other features that might be considered for alternative interpretations for the traces documented in the Usclas Formation (**Figure S4**).

The table (following pages) describes each photo (A-I; with references cited) and summarizes discrepancies with the features of the Usclas Formation.

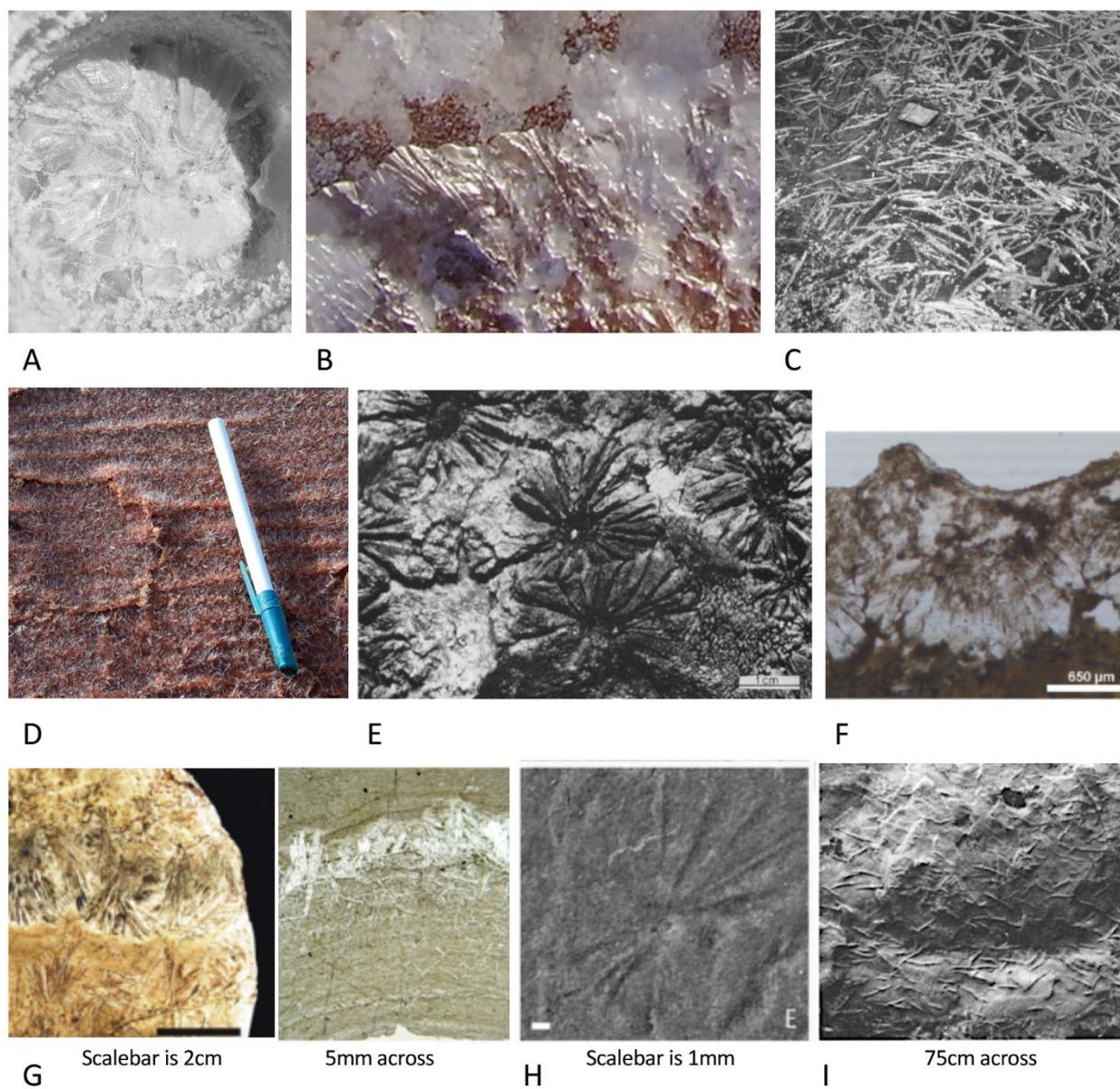



Figure S3

Photo description	Discrepancies
(A) Feathery halite grown at air-water interface in beaker (unpublished, from K. Benison, 2020)	Feathery halite grows at the air-water interface, whereas all Usclas Fm. features formed displacively (grew into the fine sediment, pushing it aside). Also, individual needles are finer and more well-defined in the Usclas <i>FN</i> features (compared to sheetlike form of the feathery halite, wherein individual needles are poorly-defined and concave).
(B) Feathery halite growing at the edge of small brine puddles, Lake Ballard, Australia (unpublished, from K. Benison, 2020)	
(C) Floating crust of acicular thenardite crystals in playa lakes of the northern Great Plains (from Last, 1984)	Floating crusts of one (acicular) form of thenardite form at the air-water interface; Usclas Fm. features were formed displacively. The needles of acicular thenardite are also an order of magnitude larger in scale, and do not form fan-like geometries.
(D) Needle-like gypsum crystals (mm-scale) on a rippled mudflat, Lake Aerodrome, Australia (Fig. 6G from Benison and Bowen, 2013)	Major differences occur in both scale and morphology: Usclas <i>SR</i> blades are ~10x larger and exist as bunches of needles, compared to the very fine, hair-like needles of gypsum in photo (D).
(E) “Daisy bed” gypsum , Sicilian Basin (from Schreiber et al., 1976)	In contrast to these, the Usclas <i>DC</i> impressions are not consistently radial and lacks a central pore. Daisy bed gypsum in this photo (E) has fewer, and less-delicate needles.
(F) Fan-like bloedite crystals, viewed in cross-section, in saline lakes, Spain (from Mees et al., 2011)	Micromorphological characteristics are distinctly blockier or more prismatic than in the Usclas Fm.
(G) Radiating bladed fans of barite , South China (plan view Fig. 2C from Zhou et al., 2010 and cross-sectional Fig. 2C from Killingsworth et al., 2013)	Micromorphological characteristics show fuller (bulkier) fans than any Usclas Fm. morphology –In cross section, in contrast to Usclas <i>SR</i> , barite needles are more abundant and disorganized, and also extend gradationally into the matrix.
(H) <i>Palaeoscia floweri</i> , porpitiid siphonophores, Jurassic, northeastern U.S. (from Collette et al., 2011)	In contrast to these, the Usclas Fm. features lack a central pore and do not occur individually. Furthermore, their cross-sectional micromorphologies do not have a funneled shape or structureless-vuggy fill typical of burrowing (e.g., Collette et al., 2011).
(I) Rare example of randomly-oriented, spindle-like, synaeresis cracks (from Plummer and Gostin, 1981)	Usclas Fm. impressions do not form full or partial polygons (typical of desiccation, synaeresis, or freeze-thaw casts). In contrast to one rare example of randomly-oriented spindle-like synaeresis cracks, Usclas Fm. features are characterized by substantially thinner, more needle-like lines

<p>Note on Fossils</p> <p style="text-align: center;">2 cm</p> 	<p>Plant taphonomy, fauna, insects, and trackways of the Lodève Basin are well-documented (e.g. Martín-Closas and Galtier, 2005; Gand et al., 2008; Galtier and Broutin, 2008; Lopez et al., 2008), and do not resemble any of the Usclas morphologies. Small, dark fern fossils with coniferous (needle-like) leaves (<i>left</i>) were found in the same Usclas Fm. section. They represent species of <i>Walchia</i> (cf. <i>Walchianthus</i> sp.; Bercovici and Broutin, 2008), which do not match the Usclas traces in size or form—nor do they have the same preservation (e.g., organic matter).</p>
--	---

- Benison, K.C. and Bowen, B.B., 2013, Extreme sulfur-cycling in acid brine lake environments of Western Australia, *Chemical Geology*, v. 351, p. 154–167, <https://doi.org/10.1016/j.chemgeo.2013.05.018>.
- Bercovici, A. and Broutin, J., 2008, La flore autunienne du site de l'étang de Martenet étude taphonomique et implications paléoenvironnementales, *Palevol*, v. 7, n. 1–16, <https://doi.org/10.1016/j.crpv.2007.10.004>.
- Collette, J.H., Getty, P.R., and Hagadorn, J.W., 2011, Insights into an Early Jurassic dinosaur habitat: ichnofacies and enigmatic structures from the Portland Formation, Hoover Quarry, Massachusetts, USA, *Atlantic Geology*, v. 47, p. 81–89. <https://doi.org/10.4138/atlgol.2011.003>.
- Galtier, J. and Broutin, J., 2008, Floras from red beds of the Permian Basin of Lodève (Southern France), *Journal of Iberian Geology*, v. 34, n. 1, p. 57–72.
- Gand, G., Garric, J., Schneider, J., Walter, H., Lapeyrie, J., Martin, C., and Thiery, A., 2008, Notostraca trackways in Permian playa environments of the Lodève basin (France), *Journal of Iberian Geology*, v. 34, n. 1, p. 73–108.
- Killingsworth, B.A., Hayles, J.A., Zhou, C., and Bao, H., 2013, Sedimentary constraints on the duration of the Marinoan Oxygen-17 Depletion (MOSD) event. *Proceedings of the National Academy of Sciences of the United States of America*, v. 110, n. 44, p. 17686–17690, <https://doi.org/10.1073/pnas.1213154110>.
- Last, W. M., 1984, Sedimentology of playa lakes of the northern Great Plains. *Canadian Journal of Earth Sciences*, v. 21, n. 1, p. 107–125, <https://doi.org/10.1139/e84-011>.
- Lopez, M., Gand, G., Garric, J., Korner, F., and Schneider, J., 2008, The playa environments of the Lodève Permian basin, *Journal of Iberian Geology*, v. 34, n. 1, p. 29–56.
- Martín-Closas, C. and Galtier, J., 2005, Plant Taphonomy and Paleoecology of Late Pennsylvanian Intramontane Wetlands in the Graissessac-Lodève Basin (Languedoc , France). *PALAIOS*, v. 20, n. 3, p. 249–265.
- Mees, F., Castañeda, C., Herrero, J., and Ranst, E. Van, 2011, Bloedite sedimentation in a seasonally dry saline lake (Salada Mediana, Spain), *Sedimentary Geology*, v. 238, n. 1–2, p. 106–115, <https://doi.org/10.1016/j.sedgeo.2011.04.006>.
- Plummer, P.S. and Gostin, V.A., 1981, Shrinkage cracks: Desiccation or synaeresis? *Journal of Sedimentary Petrology*, v. 51, n. 4, p. 1147–1156.
- Schreiber, B.C., Friedman, G.M., Decima, A., and Schreiber, E., 1976, Depositional environments of Upper Miocene (Messinian) evaporite deposits of the Sicilian Basin, *Sedimentology*, v. 23, p. 729–760.
- Zhou, C., Bao, H., Peng, Y., & Yuan, X. (2010). Timing the deposition of 17 O-depleted barite at the aftermath of Nantuo glacial meltdown in South China. *Geology*, 38(10), 903–906. <https://doi.org/10.1130/G31224.1>